Effect of the location of Mn sites in ferromagnetic GaMnAs on its Curie temperature

K. M. Yu and W. Walukiewicz,

Center for Advanced Materials, Materials Sciences Division,
Lawrence Berkeley National Laboratory, Berkeley, CA 94720

and

T. Wojtowicz, I. Kuryliszyn, X. Liu, Y. Sasaki, and J. K. Furdyna

Department of Physics, University of Notre Dame, Notre Dame, IN 46556

ABSTRACT

We report a strong correlation between the location of Mn sites in ferrromagnetic $Ga_{1-x}Mn_xAs$ measured by channeling Rutherford backscattering and by particle induced x-ray emission experiments and its Curie temperature. The concentrations of free holes determined by electrochemical capacitance-voltage profiling and of uncompensated Mn^{++} spins determined from SQUID magnetization measurements are found to depend on the concentration of unstable defects involving highly mobile Mn interstitials. This leads to large variations in T_C of $Ga_{1-x}Mn_xAs$ when it is annealed at different temperatures in a narrow temperature range. The fact that annealing under various conditions has failed to produce Curie temperatures above ~110K is attributed to the existence of an upper limit on the free hole concentration in low-temperature-grown $Ga_{1-x}Mn_xAs$.

In recent years, there is a growing interest in the possibility of using electron spins in electronic devices for the processing, transferring, and storing of information [1]. Many of such applications would require a combination of semiconducting and magnetic properties in the same material. The prospects for the practical realization of such "spintronic" devices increased significantly when it was discovered that alloys of GaAs with Mn (specifically, $Ga_{1-x}Mn_xAs$ with $x \approx 0.07$) could be made ferromagnetic with a Curie temperature T_C as high as 110 K [2,3].

It was established experimentally that T_C in $Ga_{1-x}Mn_xAs$ increases with increasing Mn concentration x (as long as MnAs precipitates are not formed) and with the hole concentration [3]. These observations are consistent with the Zener model of ferromagnetism proposed by Dietl *et al*. [4], which predicts that

$$T_C = Cxp^{1/3}, \qquad (1)$$

where x is the mole fraction of substitutional Mn^{++} ions, p is the hole concentration, and C is a constant specific to the host material. Alternatively, it has been proposed that the ferromagnetic coupling between Mn^{++} ions is mediated by holes localized on adjacent ions [5].

It should be noted that Mn atoms can occupy three types of sites in the $Ga_{1-x}Mn_xAs$ lattice. Mn atoms can occupy the Ga lattice sites to form the $Ga_{1-x}Mn_xAs$ alloy. They can occupy *interstitial* sites commensurate with the zinc-blende lattice structure. Finally, Mn atoms can also precipitate out to form different phases (e.g., MnAs inclusions). In the latter case Mn resides at random sites and therefore it is incommensurate with the zinc blende lattice. In $Ga_{1-x}Mn_xAs$ only the substitutional Mn^{++} ions act as acceptors, so that x and p in Eq. (1) are intimately related. As all interstitials of metal atoms Mn interstitials act as donors and tend to passivate substitutional Mn acceptors. Mn atoms which form precipitates (e.g., MnAs inclusions) do not contribute

free holes, and are thus outside the Zener picture of magnetization. Therefore, to understand the limitations on the maximum T_C in $Ga_{1-x}Mn_xAs$, it is necessary to address the issue of the lattice site location of Mn, and its relation to the concentrations of both the free holes and of uncompensated Mn^{++} spins. A few studies addressing the local structures of Mn in III-Mn-V alloys using extended x-ray absorption fine structure (EXAFS) had been reported [6,7]. While accurate determination of near neighbor distances (<±0.005Å) and local disorders can be achieved using the EXAFS technique, it is not sensitive in measuring the coordination numbers (~20%) and distinguishing the chemical nature of the neighbors with small difference in atomic number (e.g. Ga and As). Lattice site location of impurities can only be indirectly inferred from multi-parameter fitting of the EXAFS spectra using calculated model structures.

In this paper we report a study of the lattice sites occupied by Mn atoms in thin $Ga_{1-x}Mn_xAs$ films using channeling Rutherford backscattering (c-RBS) and particle induced x-ray emission (c-PIXE) experiments. The results are combined with measurements (on the same samples) of the free hole concentration, carried out by the electrochemical capacitance-voltage (ECV) profiling; and of magnetization, carried out by SQUID measurements. These studies clearly establish the correlation between the arrangement of Mn sites in $Ga_{1-x}Mn_xAs$ and its Curie temperature.

The $Ga_{1-x}Mn_xAs$ films were grown on semi-insulating (001) GaAs substrate in a Riber 32 R&D molecular beam epitaxy system. Fluxes of Ga and Mn were supplied from standard effusion cells, and As_2 flux was produced by a cracker cell. Prior to $Ga_{1-x}Mn_xAs$ deposition we grew a 450 nm GaAs buffer layer at 590°C (i.e., under normal GaAs growth conditions). The substrate was then cooled down to 265°C for the growth of a 3 nm thick low-temperature (LT) GaAs, followed by a 110 nm GaMnAs layer using an As_2:Ga beam equivalent pressure ratio of 20:1. Mn concentration in the sample was estimated to be 8 ± 2% from the change in the growth rate monitored by RHEED oscillations. After the growth, three adjacent 7x7 mm pieces of the wafer were cut for

further study. One of these was used as-grown, the other two were annealed at 282°C and 350°C, respectively, for 1 hr in flowing N_2. The locations of Mn sites in the $Ga_{1-x}Mn_xAs$ lattice were then studied by directly comparing the Mn K_α x-ray signals (c-PIXE) with the c-RBS signals of GaAs from the $Ga_{1-x}Mn_xAs$ film simultaneously obtained using a 1.95MeV $^4He^+$ beam.

The T_C of the as-grown $Ga_{1-x}Mn_xAs$ film was 67K. Annealing at 282°C (i.e. at temperature only slightly higher than the growth temperature) increased the T_C to 111K. Annealing at 350°C, however, resulted in a lower T_C of 49K. It has been shown previously that varying the temperature [8] or the duration [9] of the low temperature annealing has produced similar changes of T_C.

RBS and PIXE measurements on the as-grown $Ga_{1-x}Mn_xAs$ sample reveal that the film has a Mn concentration x = 0.09, in good agreement with the value from RHEED oscillations. Figure 1 compares the PIXE spectra from the as-grown $Ga_{1-x}Mn_xAs$ film when the crystal is not aligned (random), and when it is aligned in the <110> and <111> directions. The greatly reduced Mn K_α x-ray yields in the aligned spectra indicates that a dominant fraction of the Mn atoms are shadowed by the lattice site host atoms, and therefore are not visible to the beam along the axial channel direction. The fact that for certain axial channeling projections the Mn atoms are shadowed by the Ga or As atoms indicates that the Mn atoms are in specific (non-random) sites commensurate with the lattice, but does not necessarily imply that the Mn atoms are in *substitutional* positions. One striking feature shown in Fig. 1 is that the Mn K_α x-ray yields observed in the <110> alignment are much higher than those in the <111> spectrum. This immediately suggests that the non-random Mn atoms in this sample reside in more than one *non-equivalent* lattice position.

The normalized yield for the RBS (χ_{GaAs}) or the PIXE Mn x-ray signals (χ_{Mn}) is defined as the ratio of the channeled yield to the corresponding unaligned yield. The fraction of non-random Mn, f_{nr}, can then be calculated by comparing χ_{GaAs} and χ_{Mn} from

the $Ga_{1-x}Mn_xAs$ film ($f_{nr}=(1-\chi_{Mn})/(1-\chi_{GaAs})$) [10]. The f_{nr} in the different channel projections are shown in Fig. 2.

For both the as-grown $Ga_{1-x}Mn_xAs$ film and that annealed at 282°C, the f_{nr} values are similar for the <100> and <111> projections, but show a much lower value for the <110> axial direction. This arises if some Mn atoms are visible in the <110> channel and x-rays coming from these interstitial Mn are enhanced from flux peaking effect in the <110> direction [10,11] and thus f_{nr} calculated from the χ_{Mn} does not represent the true non-random Mn fraction. For the $Ga_{1-x}Mn_xAs$ film annealed at 350°C, however, the f_{nr} values observed in all directions are similar. Moreover, f_{nr} for all the channeling directions decreases with annealing, suggesting that post-growth annealing promotes random precipitation of Mn. For the specimen annealed at 350°C we estimate that 35% of the Mn atoms form random precipitates. Although it is not possible to identify the form of these random precipitates from the present study, earlier reports on annealing of $Ga_{1-x}Mn_xAs$ or Mn-implanted GaAs suggest that the Mn removed from the ordered sites forms MnAs inclusions when the annealing takes place at temperatures higher than 300°C [12-14].

Figure 3 shows the PIXE and RBS angular scans about the <110> and <111> axes for the three $Ga_{1-x}Mn_xAs$ samples. The angular scans about the <100> directions (not shown) are similar to those about the <111> direction for all three samples. The <110> angular scans are taken along the {110} planar channel. The higher χ_{Mn} for the as-grown film and for the film annealed at 282°C observed in the <110> direction as compared to those in the <100> and <111> directions suggests that the f_{nr} of Mn atoms in these samples do not all sit in substitutional sites. Specifically, these results indicate that a fraction of these non-random Mn atoms is located at tetrahedral *interstitial* sites. Atoms in the tetrahedral interstitial positions in a diamond lattice are shadowed by the host atoms when viewed along both the <100> and <111> axial as well as the (100) and (110) planar directions, but are exposed in the <110> axial channel at two equivalent interstitial

positions parallel to the (110) plane and in the (111) planar direction [10,11,15]. This gives rise to a double-peak feature in the <110> angular scan due to the flux peaking effect of the ion beam in the channel. A double-peak feature is indeed observable in the <110> scan for the as-grown sample (indicated by the arrows) shown in Fig. 3. The fraction of these intersititial Mn can be roughly estimated to be ~ 17%, assuming that flux peaking in the <110> channel of GaAs is ~1.5 [10,11,15]. The presence of interstitials in the as-grown film is further confirmed in (110) and (111) planar channeling scans (not shown), where we observed a higher χ_{Mn} in the (111) as compared to that in the (110) planar channels. The double-peak feature is less prominent for the sample annealed at 282°C, indicating a reduced concentration of interstitial Mn in this sample. This suggests that the Mn interstitials are unstable, and precipitate out as Mn clusters and/or MnAs upon annealing. The fact that χ_{Mn} in the sample annealed at 350°C are high and nearly equal in all the three channeling scans further suggests that not only all of the intersititial Mn, but also a significant fraction of the Mn atoms originally at the substitutional (cation) sites, leave their positions to form random precipitates.

It is well known that the determination of the hole concentration in ferromagnets is complicated by the so-called *anomalous Hall effect* (AHE), characteristic of conducting ferromagnets [3,16]. To circumvent this problem, we have used the electrochemical capacitance voltage (ECV) profiling method to measure the depth distribution of uncompensated Mn acceptors in the $Ga_{1-x}Mn_xAs$ layers [17]. This method provides information on the distribution of the net space charge in the depletion region. The ECV profiling showed an increase of the net acceptor concentration from $6x10^{20}cm^{-3}$ observed in the as-grown sample to $1x10^{21}cm^{-3}$ for the $Ga_{1-x}Mn_xAs$ film annealed at 282°C [18]. The sample annealed at 350°C, on the other hand, showed practically no change in the hole concentration. We have verified the validity of the ECV method by comparing ECV and Hall measurements on (non-magnetic) heavily Be-doped LT-GaAs. The ECV results are consistently within 10% of the Hall values of free hole concentration

[19]. We can therefore assume that there are no donor levels close to the valence band and the ECV measurements reflect the free hole concentration in the $Ga_{1-x}Mn_xAs$ films.

The ion channeling and ECV results show that out of ~$2x10^{21}$ cm^{-3} Mn atoms in the as-grown $Ga_{0.91}Mn_{0.09}As$ only $6x10^{20}$ cm^{-3} can act as electrically active uncompensated acceptors. A small fraction (~ 10%) of the remaining atoms form random (or possibly coherent) Mn and/or MnAs clusters. Arsenic antisite (As_{Ga}) donors can also compensate some of the substitutional Mn acceptors. Most important, however, the PIXE results show that in the as-grown sample a significant fraction (~ 17%) of the Mn atoms reside on interstitial sites. The interstitial Mn (designated Mn_I) are highly mobile positively charged donors. They can, however, be immobilized by occupying the interstitial sites *adjacent* to the negatively charged substitutional Mn_{Ga} acceptors, thus forming Mn_I-Mn_{Ga} pairs, and rendering Mn_{Ga} inactive as acceptors.

Annealing the sample at 282°C (only slightly above the growth temperature) breaks the relatively weak Mn_I-Mn_{Ga} pairs, releasing the highly mobile Mn_I to diffuse to available substitutional sites or to form precipitates and/or clusters, thus leaving behind the substitutional Mn_{Ga}, which can then become electrically-active acceptors. Consequently the 282°C annealing leads to a higher hole concentration, $p = 1x10^{21}$ cm^{-3} and a higher concentration of Mn atoms occupying random sites. The very high hole concentration, about an order of magnitude higher than the concentration limits in p-type GaAs [20,21] indicates that the sample annealed at 282°C is still far from thermodynamic equilibrium. This is confirmed by the annealing at 350°C that drives the system towards equilibrium by removing the Mn from the electrically active Mn_{Ga} sites, to form random precipitates and/or clusters. Such mechanism has already been shown to be a driving force that limits the free hole concentration in heavily Zn doped GaAs [21]. It should be noted here that, contrary to earlier suggestions, [9] the arsenic antisite (As_{Ga}) defects are not expected to play a significant role in the annealing-induced changes, since these latter defects have been shown to remain stable up to 450°C [22].

Measurements of magnetization very nicely corroborate these results. The saturation magnetization M_s observed at 5K on a number of $Ga_{1-x}Mn_xAs$ specimens annealed at 282ºC increases by approximately a factor of 1.5 relative to the values of M_s measured on the same specimens before annealing. This clearly supports the conclusion that the low temperature annealing breaks antiferromagnetically ordered Mn_I-Mn_{Ga} pairs leading to higher concentration of uncompensated Mn spins. Note that, according to the ECV results, annealing increased the hole concentration p from *ca.* $6x10^{20}cm^{-3}$ to $1x10^{21}cm^{-3}$, by a ratio of about 1.7, in reasonable agreement with the increase in the uncompensated magnetic moments, as indicated by the behavior of M_s. Also we find that the annealing-induced increase of T_C from 67 K to 111 K scales very well with the corresponding increase in the free hole concentration. This result further confirms the assertion that the total number of the ferromagnetically coupled spins is related to the concentration of uncompensated Mn ion acceptors rather than the total number of Mn atoms.

Our results show that the large changes in the electronic and magnetic properties induced by the annealing at temperatures so close to the growth temperature can be attributed to the lattice site rearrangement of highly unstable Mn_I. The fact that our maximum T_C of 111 K is so close to the maximum T_C of 110 K reported by other groups [2,3,9] suggests the possibility that this could be a *fundamental limit* on T_C in $Ga_{1-x}Mn_xAs$ alloy system. If so, this may be the reason why similar maximum values of T_C were found in $Ga_{1-x}Mn_xAs$ with rather different values of x, ranging from 0.053 to 0.091 [3,9].

It is well known that the formation energies and thus also the concentrations of charged defects such as Mn_I donors or Mn_{Ga} acceptors are to a large extent controlled by the Fermi energy [20]. To maximize T_C one strives to increase the concentration of electrically active Mn_{Ga} acceptors, and thus also the concentration of uncompensated Mn spins. This, however, leads to a downward shift of the Fermi energy, that in turn

increases the formation energy of negatively charged defects, thus making the incorporation of new Mn_{Ga} acceptors energetically unfavorable. It is therefore reasonable to expect that there is a hole concentration limit, beyond which additional Mn can only be incorporated in the form of Mn_I donors and/or electrically inactive precipitates. Our results indicate that in the low-temperature-grown materials the maximum T_C is achieved for the hole concentration limit $p_{max} = 10^{21}$ cm^{-3}, which requires $Ga_{1-x}Mn_xAs$ with $x > 0.045$. While this value is quite large, we note that a similar hole concentration limit ($p = 8x10^{20}$ cm^{-3}) has been also found in a nonmagnetic Be doped, low temperature grown GaAs [19,23]. It should be emphasized that any detailed description of the microscopic mechanism limiting the maximum Curie temperature will have to consider the role of As antisites donors [24,25].

In conclusion, we have shown that the location of Mn sites in the $Ga_{1-x}Mn_xAs$ lattice plays a crucial role in determining its magnetic properties. The concentrations of free holes and of uncompensated Mn spins, both of which underlie the ferromagnetic properties in the $III_{1-x}Mn_xV$ alloys, are thus seen to be controlled by the behavior of unstable defects involving highly mobile Mn interstitials. In particular, the Curie temperature of $Ga_{1-x}Mn_xAs$ is clearly affected by the rearrangement of the Mn atoms in the crystal lattice. The relationship of T_C to the behavior of Mn interstitials thus leads to wide variations of this parameter for annealing even in a narrow temperature window. Finally, we note that the observed limit for maximum Curie temperature can be attributed to the limit on the free hole concentration attainable in low temperature grown $Ga_{1-x}Mn_xAs$.

This work was supported by the Director, Office of Science, Office of Basic Energy Sciences, Materials Science Division of the U. S. Department of Energy under Contract No. DE-AC03-76SF00098; NSF Grant DMR00-72897; the DARPA SpinS Program; and the 21st Century Science and Technology Fund of Indiana. One of us (T.W.) gratefully acknowledges the support of the Fulbright Foundation.

REFERENCES

1. G. A. Prinz, Science **282**, 1660 (1998).
2. H. Ohno, Science **281**, 951 (1998).
3. H. Ohno, J. Mag. Mag. Mat. **200**, 110 (1999) and references therein.
4. see e. g. T. Dietl, H. Ohno, F. Matsukura, J. Cibert, and D. Ferrand, Science, **287**, 1019 (2000).
5. L. Van Bockstal, A. Van Esch, R. Bogaerts, F. Herlach, A. van Steenbergen, J. D. Boeck, and G Borghs, Physica B, 246-247, 258 (1998).
6. Y. L. Soo, S. W. Huang, Z. H. Ming, Y. H. Kao, H. Munekata, L. L. Chang, Phys. Rev. **B53**, 4905 (1996).
7. R. Shioda, K. Ando, T. Hayashi, and M. Tanaka, Phys. Rev. **B58**, 1100 (1998).
8. T. Hayashi, Y. Hashimoto, S. Katsumoto and Y. Iye, Appl. Phys. Lett. **78** (2001) 1691.
9. S. J. Potashnik, K. C. Ku, S. H. Chun, J. J. Berry, N. Samarath and P. Schiffer, Appl. Phys. Lett. **79**, 1495 (2001).
10. L. C. Feldman, J. W. Mayer, and S. T. Picraux, *Materials Analysis by Ion Channeling* (Academic, New York, 1982).
11. J. R. Tesmer, M. Nastasi, J. C. Barbour, C. J. Maggiore, and J. W. Mayer, eds. *Handbook of Modern Ion Beam Materials Analysis* (Materials Research Society, Pittsburgh, 1995).
12. J. De Boeck, R. Oesterholt, A. Van Esch, H. Bender, C. Bruynseraede, C. Van Hoof, and G. Borghs, Appl. Phys. Lett. **68**, 2744 (1996).

13. Jing Shi, J. M. Kikkawa, D. D. Awschalom, G. Medeiros-Ribeiro, P. M. Petroff, and K. Babcock, J. Appl. Phys. **79**, 5296 (1996).

14. P. J. Wellmann, M. Garcia, J.-L. Feng, and P. M. Petroff, Appl. Phys. Lett. **71**, 2532 (1997).

15. K. M. Yu, W. Walukiewicz, L. Y. Chan, R. Leon, E. E. Haller, J. M. Jaklevic, and C. M. Hanson, J. Appl. Phys. **74**, 86 (1993).

16. L. Berger and G. Bergmann, in *The Hall Effect and Its Applications*, edited by L. Chien and C. R. Westgate (Plenum, New York, 1980), p.55.

17. M. M. Faktor, T. Ambridge, C. R. Elliot, J. C. Regnault, Current Topics in Materials Science, Amsterdam: North Holland vol. 1, p. 1 (1980).

18. Similarly large values of hole concentration have been obtained in carbon-doped GaAs (see e. g.. Yamada *et. al.*, J. Crystal Growth **95**, 145 (1989)).

19. K. M. Yu et al., unpublished (2001).

20. W. Walukiewicz, Appl. Phys. Lett. **54**, 2094 (1989).

21. W. Walukiewicz, Physica B **302-303**, 123 (2001).

22. D. E. Bliss, W. Walukiewicz, J. W. Ager, E. E. Haller, K. T. Chan and S. Tanigawa, J. Appl. Phys. **71**, 1699 (1992).

23. P. Specht, M.J. Cich, R. Zhao, N.D. Jäger, J. Gebauer, F. Börner, R. Krause-Rehberg, M. Luysberg, E.R. Weber, in: *2000 Int. Semiconducting and Insulating Materials Conference, SIMC-XI*, eds.: C. Jagadish, N.J. Welham, (EEE Publ. 2001) p.73.

24. B. Grandidier, J. P. Nys, C. Delerue, S. Stiévenard, Y. Higo, and M. Tanaka, Appl. Phys. Lett. **77**, 4001 (2000).

25. S. Sanvito and N. A. Hill, Appl. Phys. Lett. 78, 3493 (2001).

FIGURE CAPTIONS

Fig. 1 PIXE spectra from the as-grown $Ga_{1-x}Mn_xAs$ film when the crystal is not aligned (random) and aligned in the <110> and <111> directions.

Fig. 2 The non-random fractions of Mn for the three different $Ga_{1-x}Mn_xAs$ films as calculated from the values of χ_{GaAs} and χ_{Mn} in the different channel projections.

Fig. 3 Angular scans about the <110> and <111> axes for the three $Ga_{1-x}Mn_xAs$ samples. The <110> angular scans are taken along the {110} planar channel.

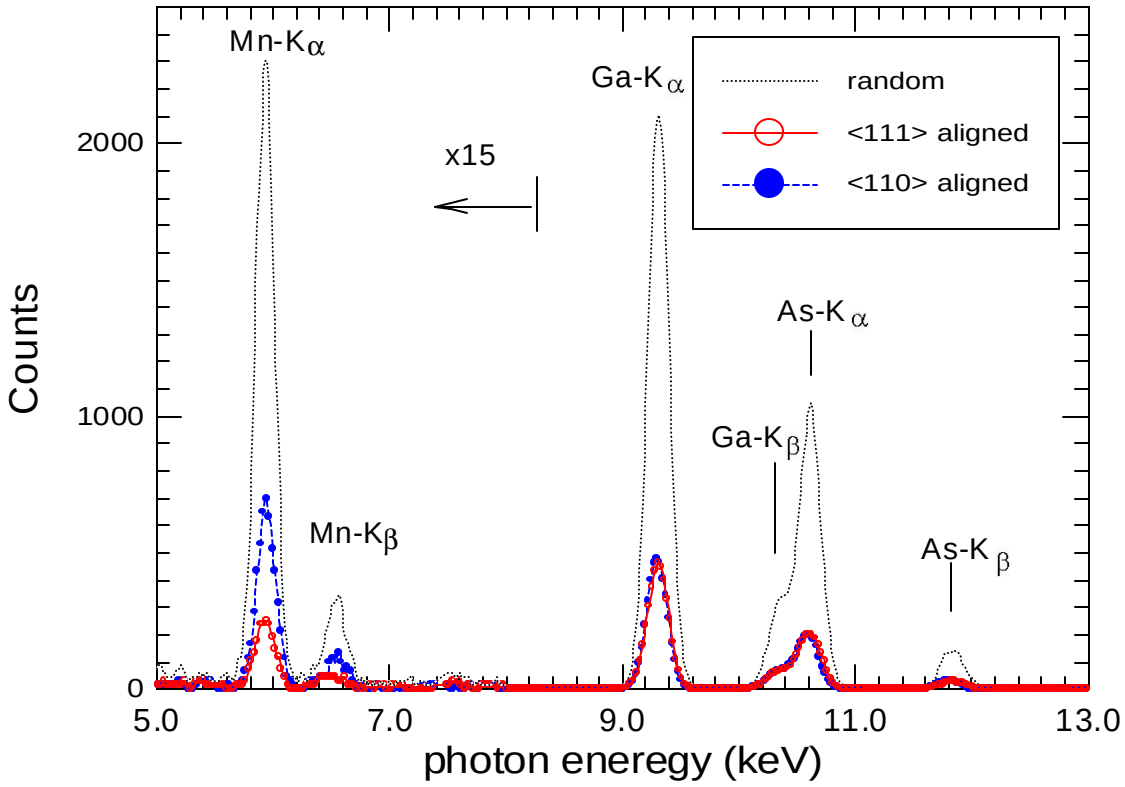
Mn-Kα
Ga-Kα
random
<111> aligned
<110> aligned
x15
As-Kα
Ga-Kβ
Mn-Kβ
As-Kβ
Counts
2000
1000
0
5.0
7.0
9.0
11.0
13.0
photon eneregy (keV)

Fig. 1

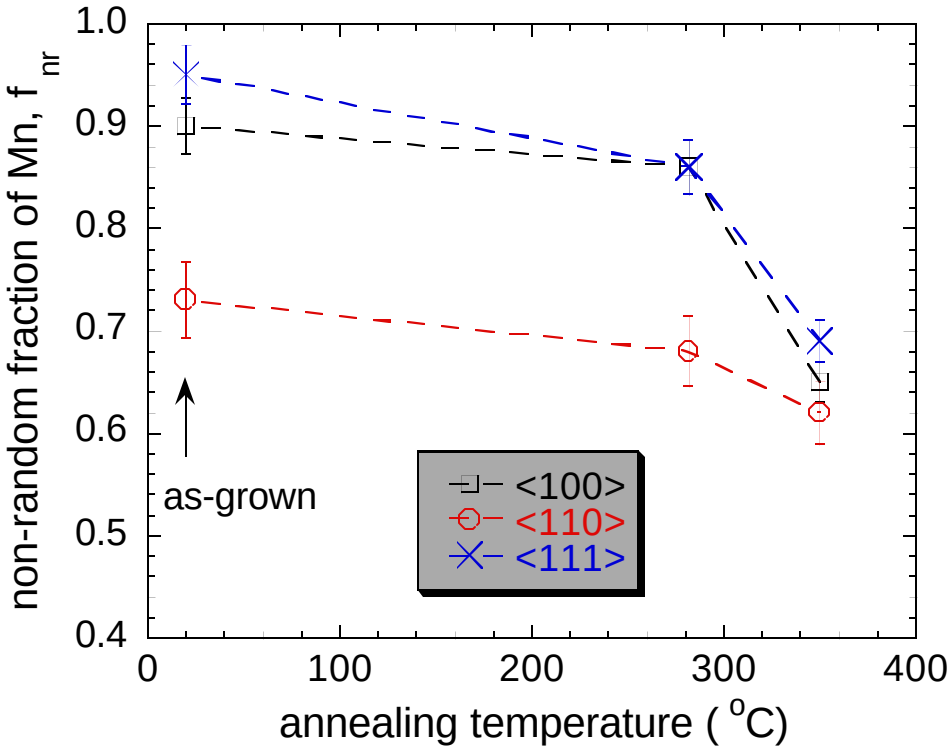
1.0
0.9
0.8
0.7
0.6
0.5
0.4
non-random fraction of Mn, f nr
0
100
200
300
400
annealing temperature (oC)
as-grown
<100>
<110>
<111>

Fig. 2

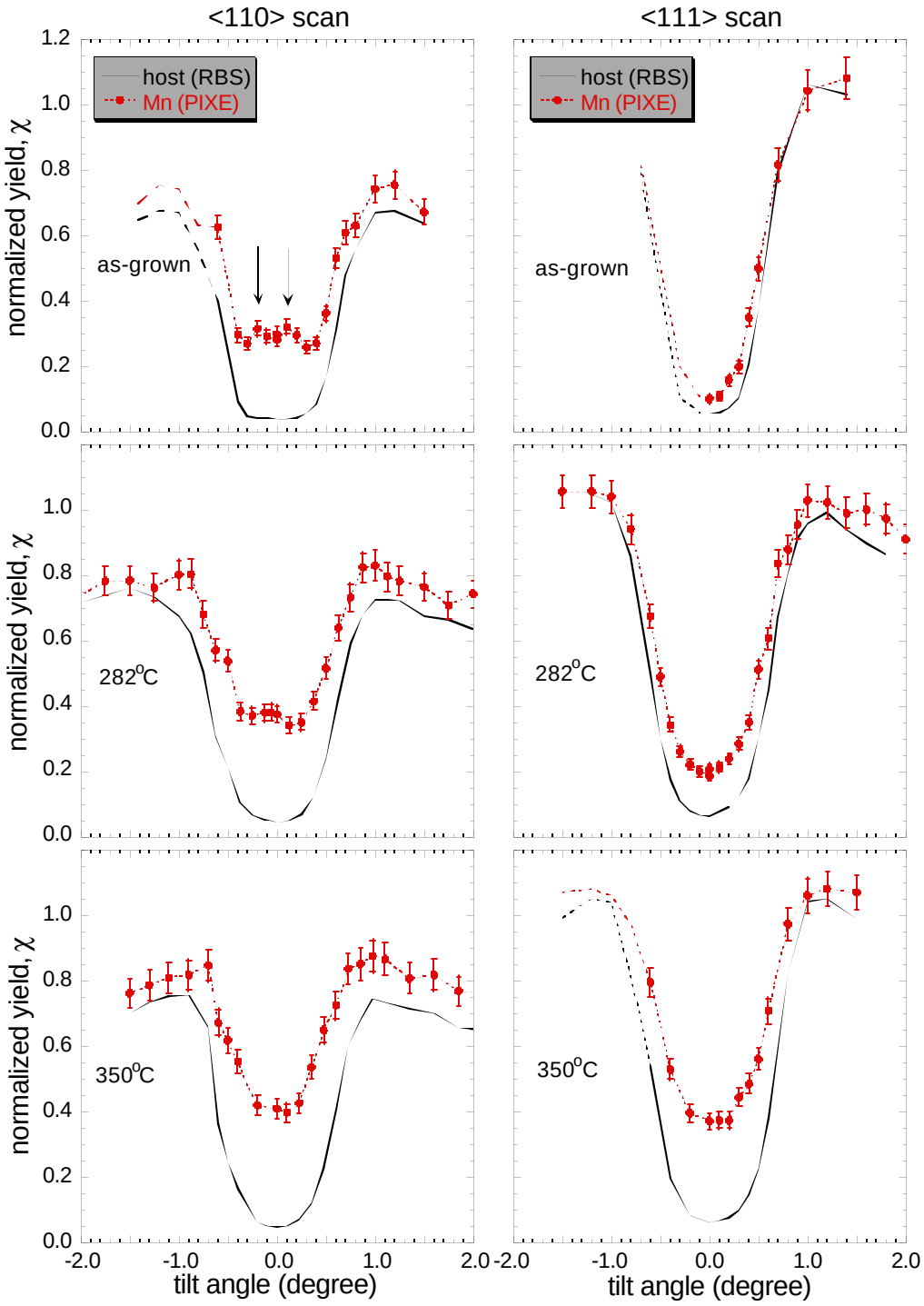
<110> scan
<111> scan
host (RBS)
Mn (PIXE)
as-grown
282°C
350°C
normalized yield, χ
tilt angle (degree)
1.2
1.0
0.8
0.6
0.4
0.2
0.0
-2.0
-1.0
0.0
1.0
2.0

Fig. 3